Candida albicans isolates contain frequent heterozygous structural variants and transposable elements within genes and centromeres

Ursula Oggenfuss, Robert T Todd, Natthapon Soisangwan, et al.

Genome Res. published online October 22, 2024
Access the most recent version at doi:10.1101/gr.279301.124

Candida albicans isolates contain frequent heterozygous structural variants and transposable elements within genes and centromeres

Authors

Ursula Oggenfuss[1], Robert T. Todd[1,2], Natthapon Soisangwan[1], Bailey Kemp[1], Alison Guyer[1], Annette Beach[1], Anna Selmecki[1,#]

1 Department of Microbiology and Immunology, University of Minnesota, Minneapolis, MN, USA

2 Department of Biology, Bard College, Annandale-on-Hudson, New York, NY, USA

#Corresponding author:

Anna Selmecki, PhD

Phone: 612-625-2263

FAX: 612-626-0623

E-mail: selmecki@umn.edu

ORCiD: 0000-0003-3298-2400

Running title: Structural variants in a human fungal pathogen

Abstract

The human fungal pathogen *Candida albicans* poses a significant burden on global health, causing high rates of mortality and antifungal drug resistance. *C. albicans* is a heterozygous diploid organism that reproduces asexually. Structural variants (SVs) are an important source of genomic rearrangement, particularly in species that lack sexual recombination. To comprehensively investigate SVs across clinical isolates of *C. albicans*, we conducted long read sequencing and genome-wide SV analysis in three distantly related clinical isolates. Our work included a new, comprehensive analysis of transposable element (TE) composition, location and diversity. SVs and TEs are frequently close to coding sequences and many SVs are heterozygous, suggesting that SVs might impact gene and allele-specific expression. Most SVs are uniquely present in only one clinical isolate, indicating that SVs represent a significant source of intra-species genetic variation. We identified multiple, distinct SVs at the centromeres of Chromosome 4 and Chromosome 5, including inversions and transposon polymorphisms. These two chromosomes are often aneuploid in drug resistant clinical isolates, and can form isochromosome structures with breakpoints near the centromere. Further screening of 100 clinical isolates confirmed the widespread presence of centromeric SVs in *C. albicans*, often appearing in a heterozygous state, indicating that SVs are contributing to centromere evolution in *C. albicans*. Together, these findings highlight that SVs and TEs are common across diverse clinical isolates of *C. albicans* and that the centromeres of this organism are important sites of genome rearrangement.

Introduction

Genomes are under constant evolutionary pressure from environmental stressors. Populations with higher amounts of standing genetic variation, including single nucleotide polymorphisms and structural variants (SVs), adapt more quickly than those with lower standing genetic variation (Feurtey et al. 2023). SVs consist of deletions, insertions, translocations, duplications, inversions and complex

rearrangements, including chromosomal fission and fusion events. A special type of SVs are transposable elements (TEs), mobile genomic sequences that can autonomously create new copies of themselves. SVs can induce reorganization of the genome resulting in the disruption, loss, reordering or duplication of genes (Hartmann et al. 2017; Yang et al. 2019; Fouché et al. 2023). SVs can influence gene expression, for example by the insertion or deletion of regulatory elements upstream of a gene (Butelli et al. 2012). Deleterious SVs are typically eliminated from populations by strong purifying selection (Elyashiv et al. 2010). SVs that are neutral or slightly deleterious can persist in a population for a long period of time via genetic drift (Berdan et al. 2021; Hartmann 2022). Occasionally, SVs are advantageous in a specific environment even when they are heterozygous (Lucek et al. 2019; Hämälä et al. 2021; Massonnet et al. 2022). Several examples of SVs caused by TE activity highlight how genome structure and function is strongly altered via SVs. For example, TE insertions in the promoter region of a gene encoding a major facilitator superfamily protein in a plant fungal pathogen led to increased resistance to antifungal drugs (Omrane et al. 2015, 2017). Similarly, in the same pathogen, chromosomal rearrangements likely caused by TEs led to an advantageous deletion of a gene encoding for an effector, which was likely recognized by the host (Hartmann et al. 2017). Overall, SVs encompass diverse recombination mechanisms, including TE mobilization or homologous repair following DNA-double stranded breaks (Todd et al. 2019, Berdan et al. 2021).

The human fungal pathogen *Candida albicans* is an asexual diploid organism that displays significant genomic plasticity (Vande Zande et al. 2022). SVs are important drivers of genome evolution and clinical isolates contain chromosome-level polymorphisms leading to karyotype variability (Rustchenko-Bulgac 1991; Navarro-García et al. 1995; Selmecki et al. 2005). Stress increases genome plasticity in *C. albicans* (Forche et al. 2011, 2018). For example, antifungal drug exposure, oxidative stress, and elevated temperature increase the rate of loss of heterozygosity (Forche et al. 2011, 2018). Indeed, nearly 50% of azole drug resistant clinical isolates have one or more aneuploidy (Selmecki 2006). The most common aneuploidy across diverse isolates is a duplication of the left arm of Chr 5 in an isochromosome structure, called i(5L) (Selmecki et al. 2006; Butler et al. 2009; Hickman et al. 2013;

Harrison et al. 2014; Ford et al. 2015; Ropars et al. 2018). i(5L) contains two genes involved in antifungal resistance, *ERG11*, encoding the azole drug target, and *TAC1*, encoding a transcriptional activator of drug efflux pumps (Selmecki et al. 2008; Vanden Bossche et al. 1994; White et al. 1998). Recently, we identified an isochromosome that contains two copies of the right arm of Chr 4, i(4R), that also provides a fitness benefit in the presence of azole drugs (Todd et al. 2019). These isochromosomes arise in diverse genetic backgrounds of *C. albicans* during adaptation to azole drugs (Selmecki et al. 2009; Todd et al. 2020; Todd et al. 2023). Importantly, the breakpoints of both i(5L) and i(4R) are located near the centromere of each respective chromosome (Selmecki et al. 2006; Todd et al. 2019). These two centromeres contain long inverted repeat sequences that are likely involved non-allelic homologous recombination resulting in the isochromosome structure (Sanyal et al. 2004; Burrack et al. 2013; Todd et al. 2019).

Centromeres faithfully segregate chromosomes during cell division. Within the fungi, centromeres range from point centromeres in *Saccharomyces cerevisiae*, to epigenetically defined regional centromeres that range from short (<20 kb) to long (>20 kb, *Cryptococcus neoformans)* (Meraldi et al. 2006). *C. albicans* has short (~3-4.5 kb), regional, epigenetically-marked centromeres, composed of a central core sequence surrounded by pericentromeric regions (Sanyal et al. 2004; Baum et al. 2006; Mishra et al. 2007; Ketel et al. 2009; Koren et al. 2010; Chatterjee et al. 2016; Freire-Benéitez et al. 2016). The central core sequence is dominated by the presence of the centromere-specific histone H3 variant Cse4p/CENP-A, while the pericentric sequence is dominated by normal histone H3 (Burrack et al. 2011). Centromeres frequently harbor repetitive sequences and complex chromatin structures that make the centromere especially susceptible to double-stranded breaks and erroneous repair (Croll et al. 2013). In many organisms, centromeres show sequence similarity to each other and contain centromere-specific repeats (Talbert et al. 2004). However, the eight centromeres of *C. albicans* lack conserved sequences and have likely undergone multiple rearrangements (Guin et al. 2020; Sanyal et al. 2004). Several centromeric regions in *C. albicans* and *C. dubliniensis* contain unique inverted repeats (Padmanabhan et al. 2008; Todd et al. 2019; Burrack et al. 2016). Given the repeats and erroneous repair

around centromeres we hypothesize that there is undetected variation in the centromeric regions of *C. albicans* that might further contribute to chromosome and genome plasticity of *C. albicans*.

The TE content of *C. albicans* and other yeast species is low compared to other eukaryotes (Maxwell 2000; Wells and Feschotte 2020). 63 TE families or TE fragments (*i.e.*, solo-LTRs) were previously identified in *C. albicans* in an earlier and more fragmented version of the reference genome (Goodwin and Poulter 2000; Goodwin 2001). Most TE families have only a few copies in the current version of the reference genome, and a few of the previously reported families are not detectable in the current version. *C. albicans* TE families include DNA transposons and retrotransposons with LINE and LTR-retrotransposons (Wicker et al. 2007). LTR-retrotransposons contain long terminal repeats (LTR) on each side of the element, which can undergo ectopic recombination, removing the majority of the retrotransposon and leaving only a solo-LTRs (Devos et al. 2002). There are 36 described solo-LTRs in *C. albicans*, 21 of which are not associated with an existing full-length LTR-retrotransposon (Goodwin and Poulter 2000; Goodwin 2001). The presence of solo-LTRs indicates a previously active full-length element, but solo-LTRs themselves are not fully functional or active anymore. The DNA transposon *Cirt2* and the LTR-retrotransposon *Tca2* are expressed in *C. albicans* (Matthews et al. 1997; Potocki et al. 2019). However, it is not clear whether TE expression is sufficient to generate new insertions, or if new TE insertions can remain over longer periods of time. Regardless, TEs do remain in the species, and it is not clear what role TEs play in this species. Importantly, no prior study has used long reads to determine precisely how many TE copies exist, where TEs are located in different clinical isolates, and how TEs might impact genome structure of *C. albicans*.

In addition, the mechanisms and sources of SVs are understudied. Conventional methods of SV characterization rely on extensive molecular experiments, which are limited to a few loci at the time, or short read sequencing alignments that do not reliably detect most SVs (Mahmoud et al. 2019). Short read sequencing data underestimates SVs longer than the read length and has a limited ability in determining the genomic positions, zygosity or allele frequencies of SVs. Additionally, mapping of short

read data to the reference genome has further limited the ability to determine the precise location and structure of many SVs, especially those found multiple times in the genome, like TEs.

Here, we describe the first long read sequencing analysis of three diverse clinical isolates of *C. albicans* to assess the genome-wide distribution and zygosity of SVs. We combine multiple analysis tools to improve the detection and confirmation of structural variants, transposable elements, and transposable element remnants as well as the zygosity state, with a focus on the pericentromeric regions.

Results

De novo long read genome assembly indicates the presence of large-scale C. albicans rearrangements

To conduct genome-wide analyses of structural variants, we generated Oxford Nanopore long read sequencing data for the reference isolate SC5314, along with two additional clinical isolates, L26 and P75063. These isolates are euploid and comprise two distantly related *C. albicans* clades (SC5314 and L26 in clade I and P75063 in clade SA; Hirakawa et al. 2015). Well-characterized phenotypic data and Illumina short read genome sequences are available for these isolates (Hirakawa et al. 2015). Furthermore, these isolates frequently acquire large DNA amplification events during adaptation to antifungal drug stress *in vitro* (Todd et al. 2019; Todd et al. 2023). To determine genome completeness, we conducted *de novo* genome assemblies. The *de novo* assemblies of SC5314, L26 and P75036 were fragmented into 37, 38 and 48 contigs with N50 of 1.16 Mb, 1.83 Mb and 1.03 Mb respectively (Supplemental Figure S1A). The length of largest contigs in SC5314 and L26 corresponded to the Chr 1 length described in the reference genome. We assessed the completeness of the genome assemblies using Benchmarking Universal Single-Copy Orthologs (BUSCO) (Simão et al. 2015; Manni et al. 2021). Of the 2137 Saccharomycotina BUSCO genes, 95.2%, 96.2% and 96.0% were present in SC5315, L26 and P75036 respectively, indicating a high level of completeness (Supplemental Figure S1B). Comparing the contigs to the reference genome showed large contiguity, with some potential chromosomal rearrangements and duplications found mostly in the subtelomeric regions (Supplemental

Figure S1C). These *de novo* assemblies provide a first overview of potential large-scale rearrangements and completeness.

Long read sequencing reveals frequency of structural variants

Next to *de novo* assembly, long read sequencing provides an opportunity to detect SVs through mapping to a reference genome. We mapped the long reads to the reference genome SC5314 and identified genome-wide coverage differences based on the separate MinION runs (Supplemental Figure S2A). After mapping the raw reads to the reference genome, we used DELLY and TELR for SV and TE detection and filtered for structures larger than 50 bp and identified extensive SV and TE polymorphism among all three isolates (Figure 1; 690 SVs in SC5314; 679 SVs in L26; 864 SVs in P75063). SVs and TEs that were present on only one homologue were defined as heterozygous, and SVs and TEs that were present on both homologues were defined as homozygous (Figure 1B). SVs were distributed throughout all chromosomes. Most SVs were insertions (INS; n=877), followed by deletions (DEL; n=662), translocations to another chromosome (TRA; n=126), inversions (INV; n=11), and duplications (DUP; n=9) (Supplemental Table S4). Almost all SV were heterozygous in SC5314 (95.5%), and a large number of SVs were heterozygous in L26 (75.7%) and P75063 (63.2%) (Figure 1A, Figure 2A). To confirm that genome coverage had no impact on SV detection, we repeated SV detection on downsampled input, with reduced number of reads. Downsampling indicated that the coverage was sufficiently high for a reliable SV detection, even for L26 with its lower coverage (Supplemental Figure S2B). Most SVs were smaller than 100 bp, with the exception of TEs that are 500 bp or larger (Supplemental Figure S2C). Short SVs were mostly insertions or deletions. The GC content of short SVs (< 100bp) was variable and similar to the genome-wide GC content distribution (Supplemental Figure S2D). Out of 927 short SVs, 7 include homopolymers, and 87 include short tandem repeats. Additionally, short SVs are enriched at replication origins (Supplemental Figure S2E), confirming previous reports of SC5314 (Muzzey et al. 2013).

We detected and quantified TEs independently of SVs. We found more than 75% of all TEs to be heterozygous in the isolates: SC5314 (78.3%), L26 (70.9%) and P75063 (69.6%) (Figure 1A, Figure 2A). 20.1% (59 TEs) of all TE loci were identical in location across all three isolates, while another 19.4% (57 TEs) were only shared between the closely related isolates SC5314 and L26 (Supplemental Figure S2F). The high number of shared TE loci between distantly related isolates was unexpected and likely indicates that most TE insertions are ancient, at least in a heterozygous state. Shared TEs are likely identical by descent, but might have diverged via mutation accumulation. 35% of all TE loci were only detected in the more distantly related isolate P75063, indicating that some TEs might still be active (Supplemental Figure S2F). Overall, the fact that low numbers of SVs are shared even between the closely related SC5314 and L26 indicates that SVs contribute significant sequence diversity between isolates and SV formation is ongoing.

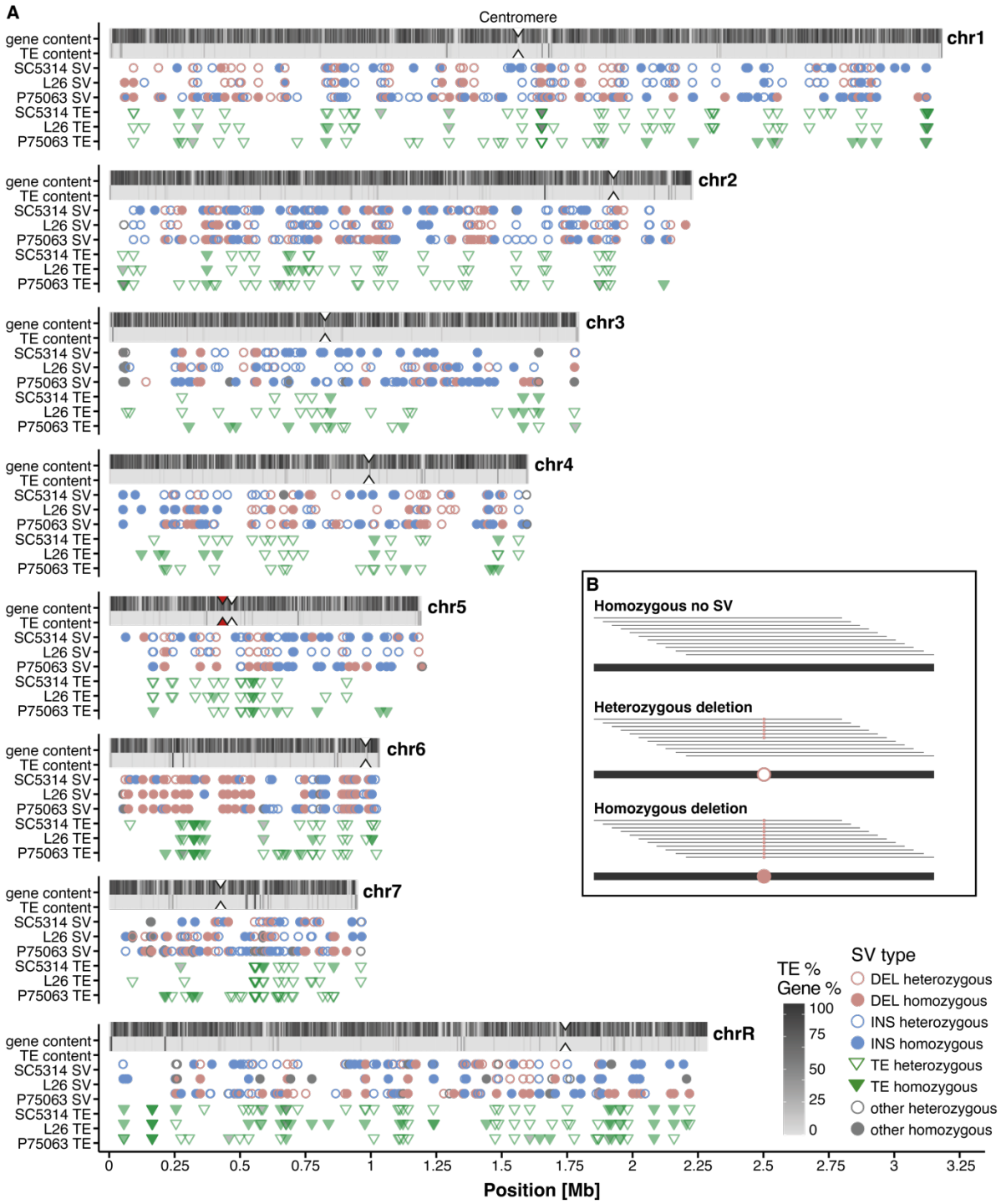

Figure 1. Long read sequencing reveals dynamic genome-wide structural variants in three clinical isolates. A) Genome-wide genomic landscape: Gene content and TE content in 5000 bp windows of the *C. albicans* reference genome. Distribution of SVs in SC5314, L26 and P75063. Colors indicate the SV type in comparison with the reference genome (green: TE = transposable element; red: DEL = deletion; blue: INS = insertion, gray = other types of SV (inversions, duplications, translocations)). The fill represents zygosity (filled symbol = homozygosity, unfilled symbol = heterozygosity). Centromeres are

marked with white notches, and the mating type locus with a red notch in Chr 5. **B)** Schematic example of heterozygous and homozygous SV definitions.

Structural variants are close to open reading frames

We next quantified the frequency of SVs within coding sequences and promoter regions. The *C. albicans* reference genome is gene dense compared to other fungal species, with a mean distance of 824 bp between annotated open reading frames (ORFs) (Supplemental Figure S2G). Given the short distance between ORFs, we defined the promoter region to be 500 bp upstream of the start codon. We scanned all annotated ORFs including a window 500 bp upstream and 500 bp downstream for overlaps with at least one SV or TE. Only 16.6% of promoter regions and ORFs contained SVs or TEs (Figure 2B). SVs and TEs in the promoter region and overlapping ORFs are predominantly heterozygous and present on only one homologue (98.7% for SVs and 91.0% for TEs in SC5314; 71.2% for SVs and 83.0% for TEs in L26; 60.6% for SVs and 73.5% for TEs in P75063).

To determine the density of SVs and TEs in genomic regions, we corrected for the length of the actual chromosomal regions defined as intergenic regions, ORFs and promoter regions. We found the highest SV and TE density in the intergenic regions, followed by the promoter region and then the ORF (Figure 2C). Due to the high gene density in *C. albicans*, SVs and TEs are generally close to ORFs, especially in the 200 bp upstream region (Figure 2D). We tested the 75 genes with a TE in the promoter or coding region for enrichment in Gene Ontology terms against a background of all *C. albicans* genes. We found a significant enrichment for the molecular function ‘3'-5' RNA helicase activity’ (p-value 0.02918). Several other genes encoding proteins involved in transport, infection, and resistance to antifungal drugs contained TEs in their promoter regions, including *ISC1*, *NSP1*, *SEC18*, *BNI4*, *CDC3*, *DYN1*, *RHO2* and *MRE11,* however these processes were not significantly enriched. The presence of TEs in the promoter region can have a significant impact on gene expression, resulting in up- or downregulation of the gene. Only a few TEs overlap with ORFs (4 in SC5314, 7 in L26 and 5 in P75063). One of these, *FMA1*, encodes a putative oxidoreductase that is associated with fluconazole resistance

(Rogers & Barker 2003). *FMA1* contains a heterozygous insertion of *Tca7* in SC5314 and the corresponding *Tca7* derived solo-LTR *zeta* in L26. These TEs likely disrupt the function of *FMA1*, but the TE copy in L26 subsequently underwent ectopic recombination. SVs and TEs are likely deleterious when located in an ORF or promoter region, but the effect could also be beneficial and generate novel functionality.

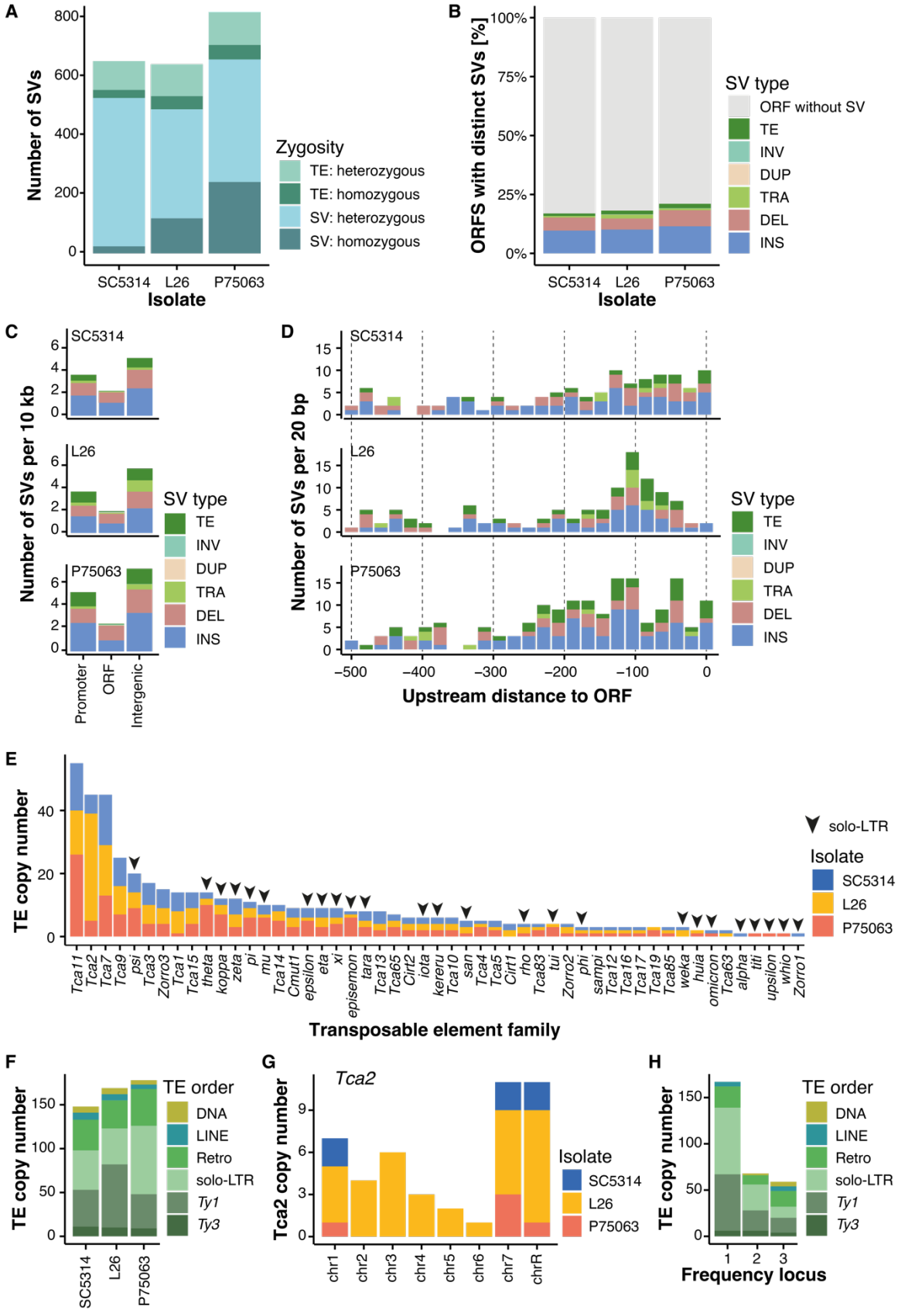

230

Figure 2. Genome-wide distribution of SVs. A) Zygosity of SVs and TEs. The bar plot represents the copy number and zygosity for SVs and TEs in the three isolates. **B)** ORFs close to SVs and TEs: Color indicates the percentage of ORFs that either overlap with at least one SV or TE, or that have at least one SV or TE in a 500 bp window upstream or downstream of the ORF. Gray indicates that no SV or TE is present. Color by SV type or TE (TE = transposable element; INV = inversion; DUP = duplication; TRA = translocation from another chromosome; DEL = deletion; INS = insertion). **C)** SVs and TEs by distance to the ORF: location in the promoter region (500 bp upstream of the ORF), overlapping with the open reading frame (ORF), or intergenic. Color by SV type or TE. Corrected by the number SV per 100 kb, as the three different regions cover space of different lengths. **D)** Fine-scale SV and TE distribution in the promoter region (500 bp upstream of the ORF). Color by SV type or TE **E)** Frequency of TE families between the three isolates. A triangle indicates this element is a solo-LTR. The sequences and their corresponding full-length elements can be found in Supplemental Table S1. **F)** TE copy numbers in the three clinical isolates. Colors indicate the classification (*Ty1* and *Ty3* are superfamilies in the LTR-retrotransposons; DNA and retrotransposon on the class level; LINE is the order of non-LTR retrotransposons; solo-LTR are fragments of *Ty1* or *Ty3* and unknown retrotransposons). **G)** Copy number of the *Tca2* transposon on each of the *C. albicans* chromosomes. Colors indicate the isolate. **H)** Frequency distribution of TE loci that are identical in location between the three isolates. Colors indicate the classification.

Indication of recent TE activity

To estimate recent TE activity, we fine-tuned our insertion and deletion polymorphism analysis, as well as the zygosity state of TEs. Within the three isolates we detected 480 TE copies belonging to 51 TE families (out of the 63 families previously identified in *C. albicans*; Goodwin and Poulter 2000; Goodwin et al. 2001) (Figure 2E). 153 of the full-length TEs belonged to the superfamily *Ty1*, followed by unclassified retrotransposons (n=94), *Ty3* (n=30), LINE/L1 (n=20) and DNA transposons (n=19) (Figure 2F). 164 TE copies were solo-LTRs, either belonging to *Ty1* or *Ty2* (Figure 2E&F). Solo-LTRs are fragments that remain after ectopic recombination of the two LTRs of a retrotransposon (Supplemental Figure S5D). The highest number of TEs was detected in the isolate P75063 (n=173), followed by L26 (n=164) and SC5314 (n=143). P75063 also had the highest number of solo-LTRs (n=78) compared to SC5314 (n=45) and L26 (n=41). L26 had an increased number of *Tca2* retrotransposons (n=34) compared to SC5314 which belongs to the same clade (n=6) and P75063 (n=5). Copies of *Tca2* were present on every chromosome in L26, while *Tca2* copies were restricted to Chr 1, Chr 7, and Chr R in SC5314 and P75063 (Figure 2G). The corresponding solo-LTRs *gamma* from *Tca2*

were not detected in any isolate. Because new TE insertions are perfect copies and mutations only slowly accumulate over time, a high sequence similarity between TE copies indicates recent activity. To determine sequence similarity, we conducted multiple sequence alignment with all *Tca2* copies from the three isolates. Overall, all *Tca2* copies showed high sequence similarity of more than 99.5%, ranging between 0 and 14 single nucleotide polymorphisms compared to the *Tca2* consensus sequence (Supplemental Figure S3A & S3B). Our data indicates recent activity of *Tca2* in the species, yet it remains unclear why and how *Tca2* increased copy numbers in L26 and not in the other two isolates.

We next tested if any TE copies were identical in location and likely ancestral. TEs were clustered into 294 individual loci, of which 167 were only present in one isolate, 68 were shared between two isolates, and 59 were shared by all three isolates (Figure 2H). DNA transposon loci generally were present in all three isolates. We found the distance to the closest ORF to be highly variable between TE families with a range from 0 to 5282 bp (Supplemental Figure S3C). The same TE families almost always had a similar range of distance to the closest ORF. Yet, while copies of *Tca2* were located close to genes in SC5314 and P75063 (range 0 to 667 bp, mean 103 bp), the copies in L26 showed a significantly higher distance (range 0 to 942 bp, mean 221 bp). This indicates relaxed selection on new TE copies inserted into gene-poor niches. Once activated, several new TE insertions may emerge. Increases of copy numbers of single TE families indicates ongoing and autonomous TE activity, yet at a much smaller scale compared to other fungal species where bursts can create hundreds to thousands of new copies (Badet et al. 2020; González-Sayer et al. 2022).

Heterozygous inverted centromere orientation and evidence of transposon activity at CEN4 and CEN5

We next focused on SVs and TEs that are in the pericentromeric regions. We detected SVs and TEs in 6 of the 8 pericentromeric regions, although only three (Chr 2, Chr 4, and Chr 5) contained TEs or TE fragments in or very close to the central core region (Supplemental Figure S4A). Chr 2 had a heterozygous solo-LTR *epsilon* in the central core region in all three isolates. Chr 4 had a *Cirt2* DNA transposon in the pericentromeric region, which was homozygous in SC5314 and L26, but heterozygous

290 in P75063. This *Cirt2* insertion corresponds to the annotated ORF *orf19.3830*, and is located only 51 bp
291 from the central core region of *CEN4* (Freire-Benéitez et al. 2016). Chr 5 had a heterozygous solo-LTR
292 *psi* in the central core region in both SC5314 and P75063 that was not detected in L26. To validate SV
293 and TE calls in the pericentromeric regions, we generated ribbon plots from the long reads mapped to
294 the reference genome for these regions. Chr 4 and Chr 5 were unique amongst all other chromosomes in
295 that their pericentromeric regions contained additional, larger SVs including large inversions covering
296 the central core regions of *CEN4* and *CEN5* (Supplemental Figure S4B).

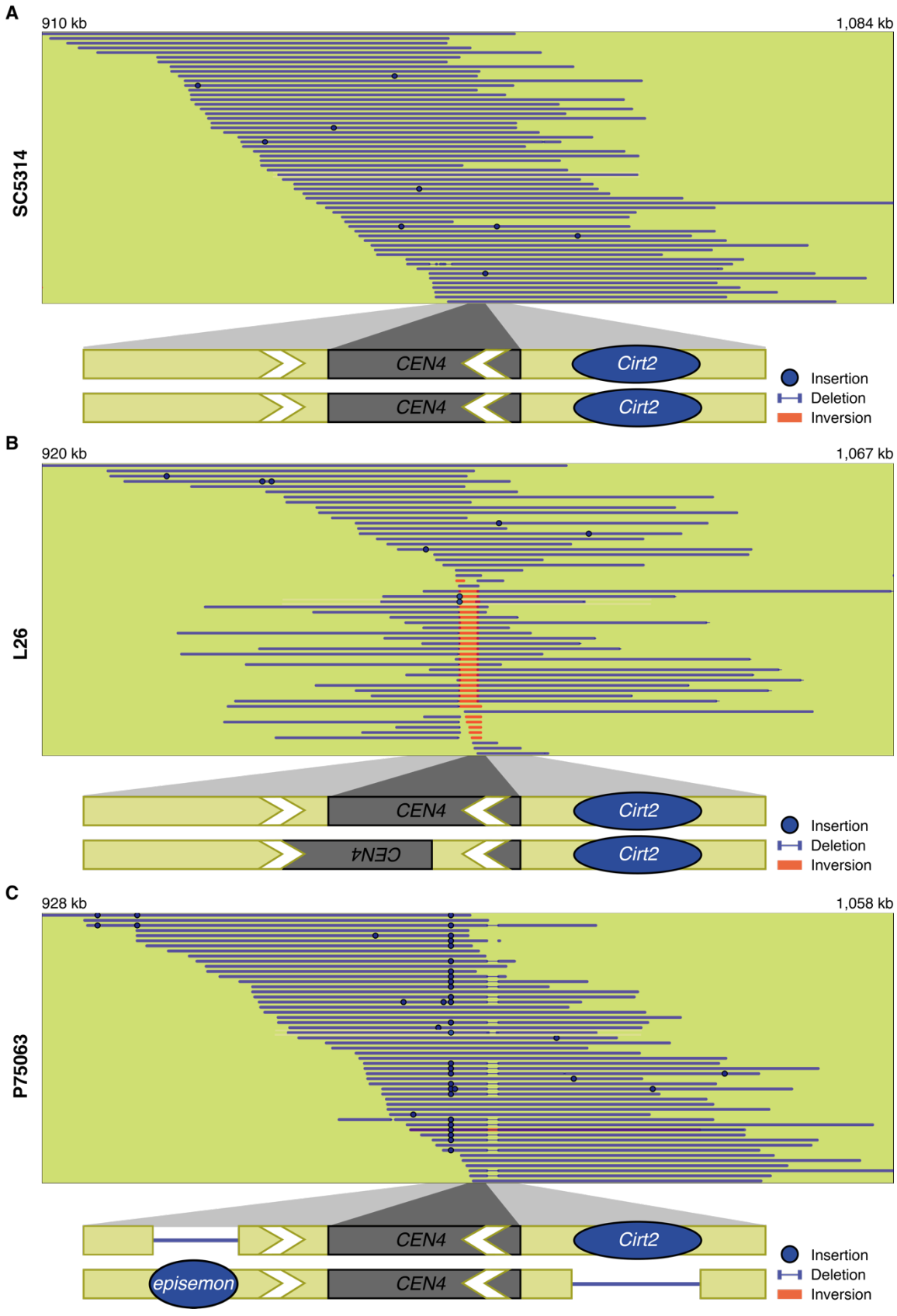

297

Figure 3. Structural variants in the pericentromere of Chr 4 in clinical isolates. Representative long reads aligned to *CEN4* in the *C. albicans* reference genome for **A)** SC5314, **B)** L26, **C)** P75063. Binding of the centromere-specific histone H3 variant Cse4p/CENP-A delineates the central core sequence of the centromere and is indicated with a gray box (Sanyal et al. 2004; Ketel et al. 2009). Blue lines indicate reads in the same orientation as the reference genome, while red reads indicate an inverted orientation compared to the reference genome. Insertions and deletions compared to the reference genome are denoted with blue dots or a thinner blue line respectively. Insertions that are not shared by more than one reads are considered to be sequencing errors. The schematic at the bottom represents a model of the *CEN4* structure (lengths not to scale). Blue circles indicate the presence of a TE. White arrows indicate inverted repeat sequences identified previously (Selmecki 2006; Todd et al. 2019).

The pericentromere of Chr 4 contained multiple SVs between the isolates. All SC5314 reads mapped to the *CEN4* region in the reference orientation and showed no indication of structural variants (Figure 3A). In L26, only half of the reads mapped to *CEN4* in the reference orientation and the other half contain an inversion of the *CEN4* sequence (Figure 3B). In P75063, all reads mapped to the *CEN4* reference orientation, however approximately half of the reads contained a 523 bp insertion upstream and an 1,824 bp deletion downstream of the *CEN4* sequence compared to the reference genome (Figure 3C; Supplemental Figure S5A). The same long reads carrying the insertion were also carrying the deletion, indicating that both SVs were phased on the same homolog. When inspecting the sequences, we found that both the insertion and the deletion correspond to TEs described in the literature in *C. albicans* (Goodwin and Poulter 2000; Goodwin et al. 2001). The insertion polymorphism belongs to *episemon*. *Episemon* is a solo-LTR with no described full-length retrotransposon in *C. albicans*, and *episemon* only had one copy in SC5314 and L26 in the pericentromeric region of Chr 5, yet 4 additional copies in different genomic locations in P75063. The deletion contains the annotated *orf19.3820* and corresponds to the full-length DNA transposon *Cirt2*. *Cirt2* belongs to the superfamily *Tc1-Mariner* and contains a transposase, 46 bp terminal inverted repeats, and generally contains "TA" target site duplications upon insertion (Supplemental Figure S5B). We detected *Cirt2* to be heterozygous present in both SC5314 and L26. A potential explanation of the absence of *Cirt2* in one allele could be mobility, with the element excising and inserting elsewhere in the genome. Indeed, our TE screen identified another copy of *Cirt2* in the right arm of Chr 4 and contained the annotated *orf19.2866* (Supplemental Figure S5C). This

second copy shared a 99.89% sequence identity with the *CEN4* proximal copy. Long read analysis showed that the second copy was present in a homozygous state in SC5314 and P75063 and a heterozygous state in L26.

The pericentromere of Chr 5 contained a similar set of SVs in the three isolates. For SC5314, half the reads mapped to the *CEN5* reference sequence while the other half reads contained two insertions compared to the reference genome (Figure 4A; Supplemental Figure S6A). The first 523 bp insertion is upstream of *CEN5* and the second 470 bp insertion is located within the Cse4p binding site in *CEN5*. We found that both insertions were solo-LTRs belonging to two different retrotransposon TE families. The *CEN5*-adjacent solo-LTR belonged to the *episemon* family with no described full-length TE family in *C. albicans*. The *CEN5 episemon* is the only *episemon* locus that is shared between all three isolates. The second insertion located in *CEN5* belonged to the *psi* family, the solo-LTR of the *Tca9* TE family (Selmecki 2006). Genome-wide, we detected 3, 2 and 7 loci of *psi* in SC5314, L26 and P75063, with the *CEN5 psi* copy as the only shared copy. In each isolate, we found three copies of the full-length element *Tca9*, yet none of the sequences overlapped with the pericentromeric or central core region. Both solo-LTRs are heterozygous and were phased on the same long reads in all three isolates (Supplemental Figure S6B). All reads from L26 mapped to *CEN5* in an inverted orientation, and half of the reads had the same insertions as SC5314 that belonged to *episemon* and *psi* (Figure 4B). In P75063, the reads mapped to *CEN5* had either the two insertions *episemon* and *psi* or had an inversion (Figure 4C). Overall, short solo-LTRs seem to be persistent in the central core and pericentromeric regions, yet only in heterozygous form, while the larger DNA transposon *Cirt2* was able to persist in a homozygous form.

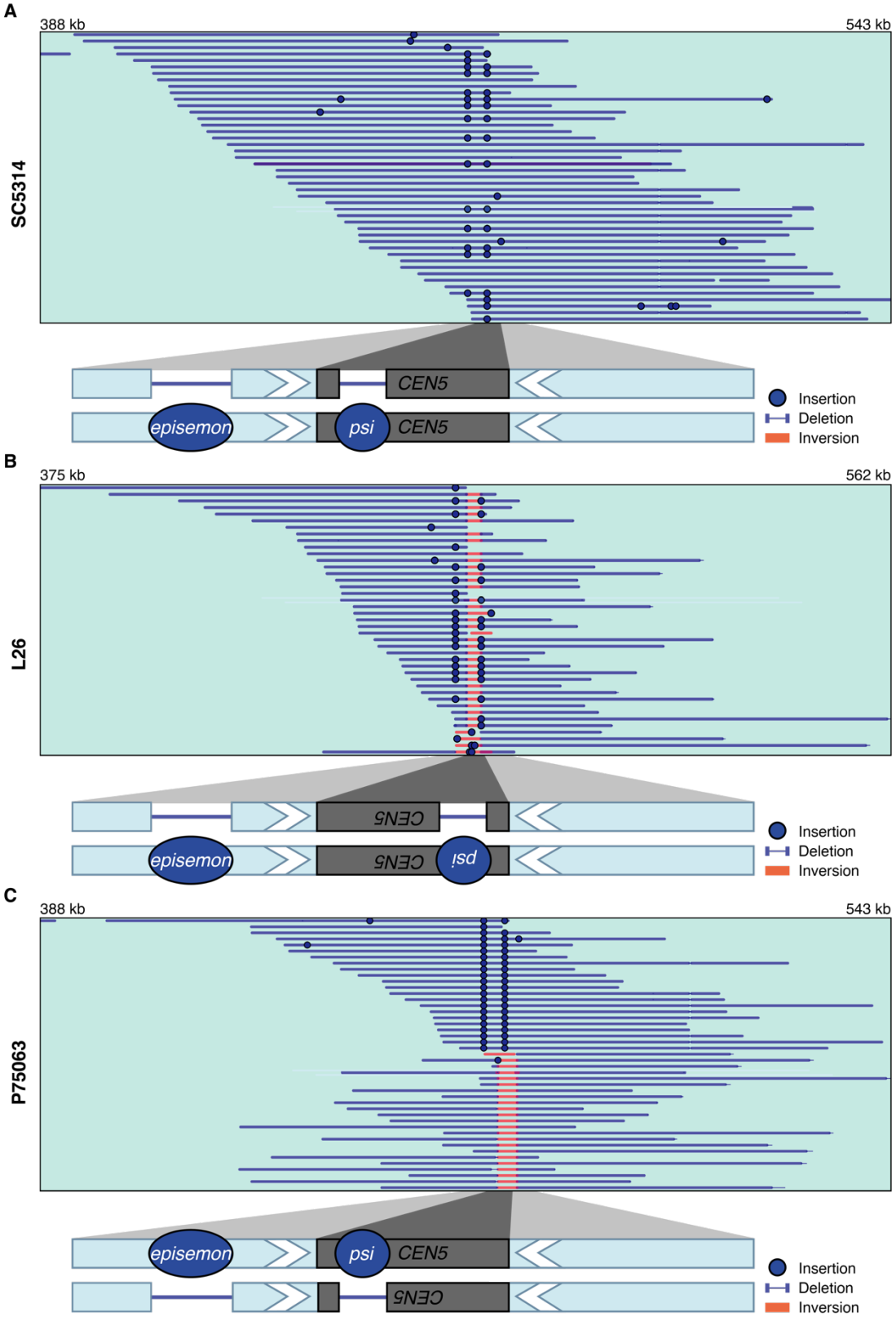

Figure 4. Structural variants in the pericentromere of Chr 5 in clinical isolates. Representative long reads aligned to *CEN5* in the *C. albicans* reference genome for **A)** SC5314, **B)** L26, **C)** P75063. Binding

of the centromere-specific histone H3 variant Cse4p/CENP-A delineates the central core sequence of the centromere and is indicated with a gray box (Sanyal et al. 2004; Ketel et al. 2009). Blue lines indicate reads in the same orientation as the reference genome, while red reads indicate an inverted orientation compared to the reference genome. Insertions and deletions compared to the reference genome are denoted with blue dots or a thinner blue line respectively. Insertions that are not shared by more than one reads are considered to be sequencing errors. The schematic at the bottom represents a model of the *CEN5* structure (lengths not to scale). Blue circles indicate the presence of a TE. White arrows indicate inverted repeat sequences identified previously (Selmecki 2006; Todd et al. 2019).

Structural variants in the pericentromeric region are frequent in clinical isolates

To determine the frequency of SVs across diverse clinical isolates, we designed PCR primers that captured the orientation and TE presence in the pericentromeric regions of *CEN4* and *CEN5* (Figure 5A&E). Then, we screened 100 *C. albicans* clinical isolates from different patients, body sites, geographic regions, and hospitals for the *CEN4* and *CEN5* SVs (Supplemental Table S2). For *CEN4* we confirmed the heterozygous inversion in L26 (Figure 5B). This heterozygous inversion was shared with 41% of the clinical isolates, while the other isolates were homozygous for the reference orientation. No instance of homozygous inversion was detected. We confirmed the homozygous presence of the pericentromeric *Cirt2* in SC5314 and L26, while the heterozygous presence in P75063 could not be confirmed, only the absence was confirmed. In the 100 clinical isolates, 41% had *Cirt2* homozygous and 9% heterozygous, while the element was absent in 50% of isolates. We confirmed the homozygous presence of the Chr 4 right arm copy of *Cirt2* in SC5314 and P75063 while the heterozygous presence in L26 could not be confirmed, again only the absence was confirmed (Figure 5D). In the 100 clinical isolates, 11% had the right arm copy of *Cirt2* homozygous state and 7% heterozygous state, while the element was not present in 82% of isolates. We did not find a correlation between the presence or absence polymorphism of the *CEN4* proximal and subtelomeric *Cirt2* copies in the 100 isolates. Likely these are independent copies (Supplemental Figure S7A&S7B).

For *CEN5*, we confirmed the *CEN5* reference orientation in SC5314, the homozygous inversion orientation in L26, and both orientations in P75063 (Figure 5F). We confirmed the heterozygous presence of the solo-LTR *episemon* in SC5314 and L26 and homozygous presence in P75063 (Figure

5G). In the 100 clinical isolates, 33% lacked an *episemon* solo-LTR, while 52% had a heterozygous and 15% a homozygous presence. In the 100 clinical isolates, 47% had a homozygous inverted orientation, 8% a homozygous reference orientation and 45% a heterozygous orientation. Finally, we confirmed the heterozygous presence of the *psi* solo-LTR (Figure 5H). In the 100 clinical isolates, 35% had a heterozygous presence for *psi*, 15% a homozygous presence and 50% showed an absence of *psi*. The *CEN5* proximal mating type locus was heterozygous in 83% of the isolates, while 6% of the loci were homozygous for *MTLa/a* and 11% homozygous for *MTLα/α* (Supplemental Figure S7C). The mating type locus and the pericentromeric SVs do not correlate and likely recombine independently (Supplemental Figure S7D). Both structural variants and TEs appeared to persist in a heterozygous state in the population. One limitation of PCR was that heterozygous TEs were difficult to capture either because one PCR product preferentially amplified better than the other (typically the smaller PCR product Figure 5C&5D, P75063 and L26 respectively) or that PCR was detecting active TE insertion/deletion events within the overnight cultures. Therefore, for the additional clinical isolates we reported simply whether a deleted TE allele amplified or not. By focusing on six structural variants in two chromosomes, we were able to detect a high variability in presence, absence and zygosity. These six structural variants seem to persist over longer evolutionary time-scales, but can also easily be lost in either one or both copies. Overall, we detected several SVs and TEs with a potential influence on chromosome stability and gene expression. Our long read sequencing and molecular validation support that SVs and TEs are frequently associated with pericentromeres in diverse C. albicans isolates. However, future experiments are needed to address the effect of SVs on C. albicans genomic plasticity and evolvability.

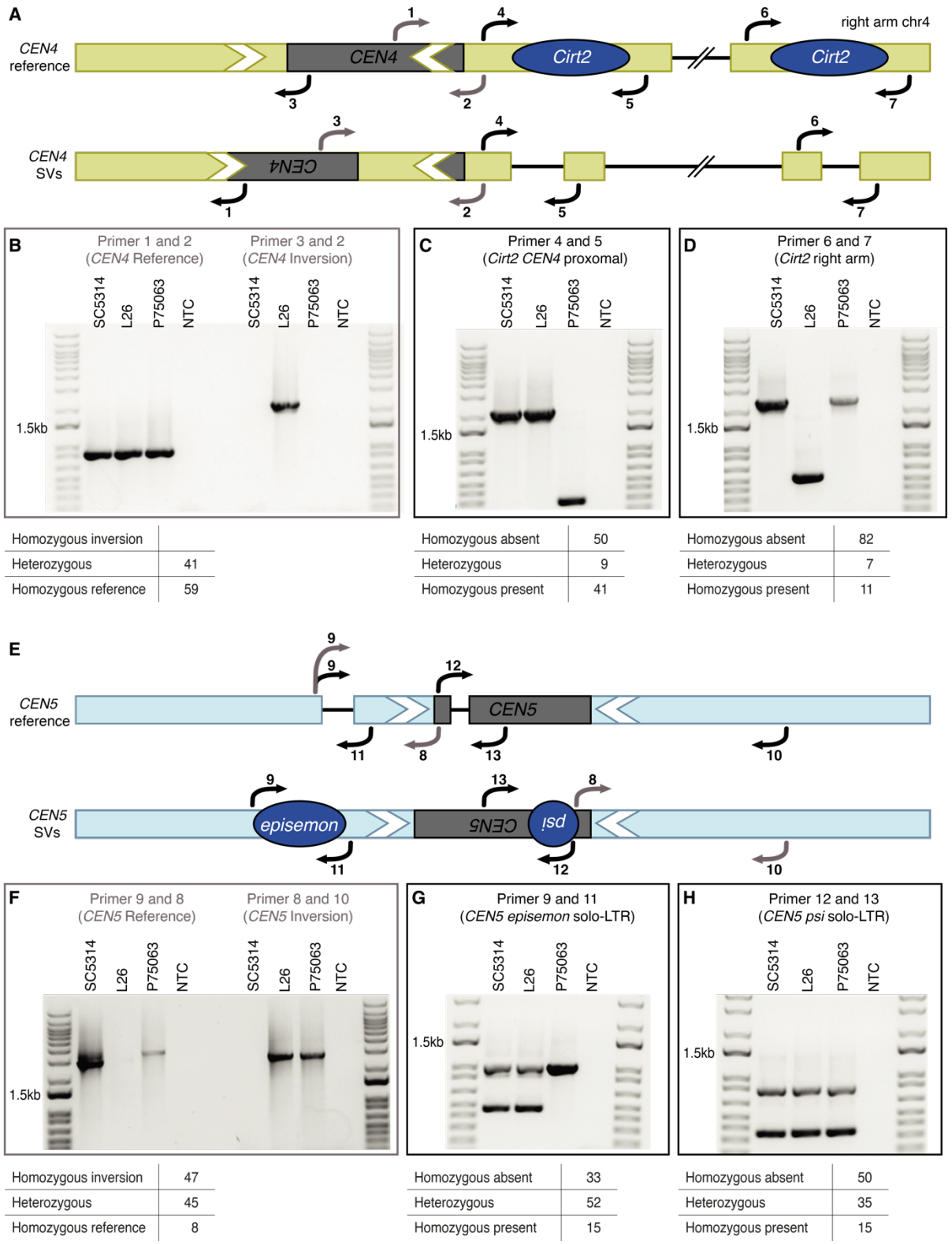

Homozygous inversion	
Heterozygous	41
Homozygous reference	59

Homozygous absent	50
Heterozygous	9
Homozygous present	41

Homozygous absent	82
Heterozygous	7
Homozygous present	11

Homozygous inversion	47
Heterozygous	45
Homozygous reference	8

Homozygous absent	33
Heterozygous	52
Homozygous present	15

Homozygous absent	50
Heterozygous	35
Homozygous present	15

Figure 5. Confirmation of centromere inversions and transposable element polymorphisms. Diagnostic PCR of *CEN4* and *CEN5* and representative strains. The table below each EtBr-stained DNA gel indicates the PCR results from 100 compiled clinical isolates. A full visualization of the 100 clinical isolates is available in Supplemental Figure S7. **A)** Schematic of the primers for *CEN4*. Cse4p/CENP-A

binding delineates the central core sequence of the centromere and is indicated with a gray box (Sanyal et al. 2004; Ketel et al. 2009). **B)** *CEN4* inversion indicated by primer pair 1 and 2 for a reference orientation, and primer pair 3 and 2 for an inversion. **C)** *CEN4* pericentromeric *Cirt2* (*orf19.3820*) presence indicated by the primer pair 4 and 5. **D)** Right arm Chr 4 *Cirt2* (*orf19.2866*) presence indicated by the primer pair 6 and 7. **E)** Schematic of the primers for *CEN5*. **F)** *CEN5* inversion indicated by primer pair 9 and 8 for a reference orientation, and primer pair 8 and 10 for an inversion. **G)** *CEN5* solo-LTR *episemon* presence indicated by the primer pair 9 and 11. **H)** *CEN5* solo-LTR *psi* presence indicated by primer pair 12 and 13.

Discussion

SVs, and TEs in particular, consist of a spectrum of genomic rearrangements, including insertions, deletions, duplications, inversions, and translocations. SVs play a crucial role in driving genome evolution, especially in asexual organisms like *Candida albicans*. Due to challenges with SV detection based on short reads, they are understudied in many species. Long read sequencing offers an exciting opportunity to detect SVs and their impact on evolution with better reliability. In this study, we provide the first analysis of SVs and TEs in three clinical isolates of *C. albicans* using long read sequencing data. We detected several SVs and TEs with a potential influence on chromosome stability and gene expression. Our specific focus on centromeres offers a unique perspective on the impact of SVs on chromosomal instability, given their important role in chromosome segregation and genome stability. We were able to detect a high variability in presence, absence and zygosity at centromere regions. Centromere structural variants seem to persist over longer evolutionary time-scales, but can also easily be lost in either one or both copies. More experiments are needed to address the effect of SVs on *C. albicans* genomic plasticity and evolvability as a fungal pathogen.

Long read sequencing improves our understanding of SV dynamics and heterozygosity

The use of long read sequencing technologies allowed us to detect a larger number of high quality SVs and TEs than previously described. We frequently found individual SVs present in only one or two isolates, and approximately half of all SVs were heterozygous. In contrast, we found a large number of TEs identical in location across all three isolates, yet almost always in heterozygous state. In other

438 species, heterozygous SVs and TEs can be deleterious, as they hinder sexual recombination (Homolka
439 et al. 2007), and consequently, most TE loci are strongly selected against, and remain at low frequencies
440 in the species (Stritt et al. 2017; Oggenfuss et al. 2021). This may not hold true in *C. albicans*, as this
441 species lacks a sexual cycle, and heterozygous SVs might not have a negative influence, but rather
442 increase the genomic plasticity and increase the potential for rapid adaptation. The heterozygous
443 presence of SVs across the genome could maintain a high level of genetic variation in the absence of
444 meiosis. Notably, *C. albicans* copy number breakpoints co-localize with SVs and repetitive regions,
445 further suggesting that the presence of heterozygous SVs could lead to chromosomal rearrangements
446 (Todd et al. 2019). SVs and TEs in particular might remain over longer periods of time by genetic drift.
447 Given the consistent presence of many TE loci, TEs cannot always be considered to be SVs in *C.*
448 *albicans*. Instead, these TEs might provide transcription factor binding sites and induce chromosomal
449 rearrangements. Finally, some SVs and TEs might have a positive impact depending on the environment.
450 For example, *FMA1* is associated with fluconazole resistance in *C. albicans* and contains a heterozygous
451 TE insertion in both SC5314 and L26. Future molecular analyses are needed to determine the effect of
452 TE insertions on drug susceptibility.
453
454 *Despite a low abundance, TEs impact genome evolution of C. albicans*
455 Previous studies show TEs cover only ~0.8% of the *C. albicans* genome, considerably less than in most
456 other eukaryotic species, but similar to other yeast species (Maxwell 2020; Wells and Feschotte 2020).
457 We found many TE loci are shared between the three *C. albicans* isolates, and they might be present in
458 other isolates or even fixed in the species. Fixation of TEs would suggest genetic drift or even a
459 beneficial impact. We detected a significant enrichment of ORFs with '3'-5' RNA helicase activity' that
460 have a TE insertion in the promoter or the ORF region. Helicases play an important role in the
461 unwinding and binding of DNA and were shown to be involved in DNA repair (Croteau et al.2020).
462 Having TE insertions in the promoter or coding region might influence the expression of helicases,
463 which could in term change the way the species responds to stress. We detected several ORFs with a

function in transport that contain a TE in the promoter region. Such TE insertions could drastically change the expression of transporter genes, potentially leading to a faster efflux of antifungal drugs and increased resistance as observed in a fungal plant pathogen (Omrane et al. 2015, 2017). Most detected TEs were heterozygous. Remaining in a heterozygous state might be a strategy for TEs to escape defense mechanisms. Additionally, the heterozygosity of many SVs and TEs upstream of ORFs might cause allele-specific expression differences that can be adaptive in changing environments.

Despite the low TE coverage, some *C. albicans* TE families are still actively expressed, even though the mechanisms that regulate and maintain their low copy numbers remain poorly understood in the species (Holton et al. 2001; Zhu et al. 2014; Potocki et al. 2019). We detected an increased copy number and a distribution to all chromosomes of the retrotransposon *Tca2* in L26, indicating that this TE might still be active. The proliferation of *Tca2* seems to be recent, and must have happened after the separation from SC5314, as SC5314 only contains 6 copies. We did not detect any copies of the solo-LTR *gamma*, indicating that no ectopic recombination has occurred. The lack of solo-LTRs supports the idea that the burst of *Tca2* in L26 was recent. Finally, the high sequence similarity of *Tca2* copies indicates that not enough time has passed to accumulate mutations. The genome-wide distribution of the *Tca2* copies suggests that the *Tca2* family is able to jump to new chromosomes, possibly via extrachromosomal intermediates (Holton et al. 2001). Therefore, our analysis suggests that TEs are likely still able to be active in *C. albicans*, although smaller in magnitude than non-yeast fungal species like the plant pathogens *Zymoseptoria tritici* or *Pseudocercospora ulei* (Badet et al. 2020; González-Sayer et al. 2022).

We detected a large number of solo-LTRs, with an increased number of solo-LTRs in P75063 compared to the other two isolates. Solo-LTRs indicate a previous insertion of the corresponding full-length retrotransposon, followed by ectopic recombination leading to the deletion of the intermediate region and one LTR, resulting in the presence of a solo-LTR (Devos et al. 2002). Similarly, ectopic recombination of two TE copies belonging to the same family will lead to the deletion of the region between the copies and one TE copy. Ectopic recombination is potentially a defense mechanism against

TE proliferation and increased genome sizes. Bird genomes that are generally compact and gene rich show a higher number of solo-LTRs as opposed to large and repeat-rich salamander genomes with low levels of solo-LTRs (Ji & DeWoody 2016; Frahry et al. 2015). *C. albicans* might use ectopic recombination of TEs as a similar strategy to birds to keep the TE content low and the genome size small. Solo-LTRs are not functional transposons, as they lack coding sequences needed for autonomous replication, and are not able to create new copies (Ma and Bennetzen 2004). However, solo-LTRs might still influence the expression of nearby genes, for example by providing transcription factor binding sites (Butelli et al. 2012). We detected several solo-LTRs of high interest that were present in all isolates in the centromeric region. The solo-LTR *episemon* was heterozygous in all three isolates in *CEN5*. Outside the pericentromeric region, only one additional copy of *episemon* was detected in P75063. However, no full-length copy of this TE is known in the literature or was detected in this study. *Episemon* does not share sequence similarity with any other known TE in *C. albicans*. This indicates that the full-length element of *episemon* likely is lost from at least the reference genome, maybe even from the species as a whole. As solo-LTRs cannot actively create new copies, *episemon* copies are likely ancient, yet remained in specific locations including the centromeres over a long period of time.

SVs and TEs in the pericentromeric region provide plasticity and adaptation potential

One observation arising from our analyses was the frequent occurrence of SVs within centromeres *CEN4* and *CEN5*. Plasticity was not only observed between centromere regions but also between different clinical isolates and between homologous chromosomes of the same isolate. We detected inversions within centromeres that are likely caused by non-allelic homologous recombination between inverted repeat sequences, and that are likely reversible (Delprat et al. 2009). We used our PCR assay as an approximation tool to estimate the general frequency of these centromere-associated features in 100 *C. albicans* clinical isolates. The presence of a frequently homozygous *Cirt2* TE near *CEN4* in multiple isolates suggests a neutral or even beneficial impact of *Cirt2*. TEs in other species are covered by facultative histone marks, which silence TEs under normal conditions, and allow expression under stress

conditions (Fouché et al. 2020). Self-regulation to keep TE copy numbers low has recently been hypothesized to be a survival strategy for certain TE families in eukaryotic genomes (Stritt et al. 2021). However, whether this strategy also applies to *C. albicans* and other yeast species, remains an open question. In some isolates, *Cirt2* is still actively expressed (MacCallum et al. 2009), and indeed we detected a nearly identical copy of *Cirt2* in the right arm of Chr 4. We found the Cse4p binding site in *CEN4* to be disrupted by the inversion event. Isolates carrying the inversion likely exhibit differences in Cse4p binding that are undetectable in our current data set. As we found no strains in either the clinical isolates screen or in directed evolution experiments with a *CEN4* homozygous inversion orientation, we suggest that a homozygous *CEN4* inversion may have a strong fitness impact, leading to purifying selection against isolates carrying inversions in both homologues.

Our findings support the high centromeric plasticity previously described in *C. albicans* (Ketel et al. 2009; Burrack et al. 2016; Barra and Fachinetti 2018). SVs are potentially contributing to genomic instability and altering recombination frequencies at centromeres. Frequent breakpoints in the pericentromeric region are also observed in tumor cells in humans and sometimes resolve into isochromosomes (Shih et al. 2023). The evolutionary and adaptive trajectories of centromere inversions and insertions of TEs remain poorly understood. Recombination events that occur at the centromeres, including the formation of isochromosomes, have been shown to be sufficient to confer resistance to antifungal drug stress (Selmecki et al. 2006, Selmecki et al. 2008; Todd et al. 2019). In particular, adaptive isochromosomes i(5L) and i(4R) have been observed in clinical isolates after exposure to fluconazole (Todd and Selmecki 2020; Todd et al. 2023). Previous work has identified that fluconazole destabilizes the centromeres in *C. albicans* through the depletion of the centromere-specific H3 histone variant, Cse4p/CENP-A (Brimacombe et al. 2019). We detected most SVs around centromeres to be heterozygous, potentially allowing fast adaptation to antifungal drug conditions, while maintaining the homolog that is adapted to environments without antifungal drug. We suggest that frequent heterozygous SVs are important in maintaining high standing genetic variation in *C. albicans*. Our findings highlight the dynamics of SVs and TEs across diverse clinical isolates of *C. albicans*, with a special focus on the

diverse pericentromeric regions. Despite their low copy numbers, TEs play an important role in genome rearrangement and centromere diversity.

Methods

Culture conditions and high molecular weight gDNA extraction

The reference isolate SC5314 (clade I) and two additional clinical isolates L26 (clade I) and P75063 clade SA) were analyzed (Supplemental Table S2; clade information from Hirakawa et al. 2015). SC5314 originated from disseminated candidiasis, L26 was isolated from a vaginal sample of a vaginitis patient from Iowa, and P75063 was isolated from a bloodstream infection in France (https://www.google.com/url?q=http://www.candidagenome.org/Strains.shtml%23SC5314&sa=D&source=docs&ust=1708627174617284&usg=AOvVaw0PdQU0MmV7UP4kZ8ajck1v; Wu et al. 2007). Previously, these isolates were whole genome sequenced using Illumina short read sequencing (Hirakawa et al. 2015). High molecular weight gDNA was extracted using the Oxford Nanopore Technologies protocol "High Molecular Weight gDNA Extracted from Yeast" (see Supplemental Methods).

Genomic landscape of the C. albicans reference genome

Genome characteristics are not uniform along the chromosomes. The *C. albicans* reference genome SC5314 A21 (from now on called *C. albicans* reference genome) A21-s02-m09-r08 obtained on October 7, 2015 from the Candida Genome Database website (CGD): http://www.candidagenome.org/download/sequence/C_albicans_SC5314/Assembly21/archive/C_albicans_SC5314_version_A21-s02-m09-r08_chromosomes.fasta.gz; Van het Hoog et al. 2007) was used as a basis for a genome-wide study of niche characteristics on gene density, transposable element (TE) density, and GC content per 5000 kb window (see Supplemental Methods) (Goodwin and Poulter 2000; Goodwin et al. 2001; Rice et al. 2000; Quinlan and Hall 2010; Li and Durbin 2009; Li et al. 2009)

Long read sequencing alignment

Long read sequencing was conducted using Oxford Nanopore MinION with R9.4.1 flow cells. Raw reads were basecalled using Guppy version 5.0.11 with the super high accuracy configuration (Wick et al. 2019). Basecalled reads were aligned to *C. albicans* reference genome using minimap2 version 2.24 and the parameter *-ax map-ont* (Li 2018). Reads were sorted and indexed, duplicated reads were removed, and remaining reads were re-indexed using SAMtools. Reads were visualized with IGV version 2.4.16 and Ribbon using "Position of primary alignment in SAM/BAM entry" as read sorting (Thorvaldsdóttir et al. 2013; Nattestad et al. 2021; https://genomeribbon.com/).

To gain a general overview on sequence similarity between the genomes, simple *de novo* assemblies were conducted using Canu, quality control was conducted with BUSCO and Quast, and a visual comparison was conducted with MUMmer (see Supplemental Methods) (Koren et al. 2017; Simão et al. 2015; Manni et al. 2021; Mikheenko et al. 2018; Kurtz et al. 2004).

Genome-wide structural variant and transposable element calling and genomic landscape

To detect structural variants (SVs), DELLY was used (see Supplemental Methods) (Li 2011a; Rausch et al. 2012). SV types are inversions (INV), duplication (DUP), translocations between chromosomes (TRA), deletions (DEL) and insertions (INS) relative to the reference genome. TE presence or absence of loci in the reference genome were confirmed based on raw reads and BLASTN, and de novo TEs were detected using the TELR pipeline (Supplemental Methods) (Camacho et al. 2009; Han et al. 2022). For each annotated ORF, the number of SVs and TEs in a 500 bp window upstream and downstream of the ORF region was extracted using BEDTools window with the parameters *-r 0 -l 500* and *-r 500 -l 0* respectively. The closest SVs and TEs upstream were detected with BEDTools closest and the parameters *-iu D b*. Each SV and TE overlap with an annotated gene was detected with BEDTools intersect and the parameter *-wao*. The distance between genes was estimated with BEDTools closest and the parameters *-iu -io -D a*. To determine if any gene functions were enriched among the genes containing TEs or containing TEs in their 500 bp upstream promoter regions, we performed Gene

Ontology (GO) analysis using the Candida Genome Database Gene Ontology Term Finder with species *Candida albicans* (http://www.candidagenome.org/cgi-bin/GO/goTermFinder) (Ashburner et al. 2000; The Gene Ontology Consortium 2000). To test if sequencing depth had an impact on SV and TE detection, a downsampling analysis was performed. The number of raw reads were reduced in steps of 10% and SV and TE detection tools were run again on the reduced sets of reads as described above.

Sequence comparison for the Cirt2 and Tca2 transposable element alleles

The sequence of the position of the 1551 bp *orf19.3820* in the pericentromeric region of Chr 4 was extracted from *C. albicans* reference genome with SAMtools faidx with adding 1,000 bp on each side. BLASTN was used to compare the region with known TE sequences in *C. albicans* (Goodwin and Poulter 2000; Goodwin et al. 2001). *orf19.3820* showed a 99.95% sequence similarity on the 1822 bp consensus sequence of the DNA transposon family *Cirt2*. Both copies of the 46 bp terminal inverted repeats were detected. *Cirt2* belongs to the TE superfamily *Tc1-Mariner* or *pogo* and class of DNA transposons. We blasted the sequence on ncbi to correctly position the transposase.

For the Tca2 TE family copies that underwent amplification in L26, phylogenetic analysis was conducted as described in Oggenfuss et al (2023; see Supplemental Methods) (Li 2011b; Wickham, 2016; R Core Team 2023; Katoh et al. 2013; Waterhouse et al. 2009; Stamatakis, 2014; Yu et al. 2017, 2018, 2020; Wang et al. 2020)

PCR screen for centromeric structural variants

To validate the presence of structural variants, PCR was performed on SC5314, L26, P75063, and an additional 100 *C. albicans* clinical isolates from diverse patients, body sites, and geographic regions (Supplemental Table S2) (see Supplemental Methods).

Data access

All raw sequencing data are available under NCBI BioProject PRJNA967712 for FASTQ (SC5314: SRR24449796; L26: SRR24449795; P75063: SRR24449794), FAST5 (SC5314: SRR29423996, L26: SRR29423995, P75063: SRR29423994). This Whole Genome Shotgun project has been deposited at DDBJ/ENA/GenBank under the following accession numbers SC5314: JBIBQR000000000, L26: JBIBQQ000000000, P75063: JBIBQP000000000ß.

Competing interest statement

The authors declare they have no competing interests.

Acknowledgements

We thank Judy Berman (Tel Aviv University) for in-depth discussions regarding the orientation of *CEN5*, and Steven Cavaliri for providing many *Candida albicans* isolates. We thank Laura Burrack (Gustavus College), Pétra Vande Zande, Xin Zhou, Dalton Piotter, Dana Davis and Nancy Scott (University of Minnesota) and the anonymous reviewers for their helpful comments on the manuscript. This work was supported by the Swiss National Science Foundation (P500PB_206850) to UO, and the National Institutes of Health (R01AI143689) and Burroughs Wellcome Fund Investigator in the Pathogenesis of Infectious Diseases Award (#1020388) to AS. The University of Minnesota Supercomputing Institute (MSI) contributed computational resources to this project.

Author contributions

AS, RTT and UO contributed to the overall study design. RTT, AG, AB, BK, and AS performed the experiments. UO and NS analyzed WGS data. The manuscript was written primarily by UO and AS with contributions from the other authors.

References

646 Ashburner M, Ball CA, Blake JA, Botstein D, Butler H, Cherry JM, Davis AP, Dolinski K, Dwight
647 SS, Eppig JT, et al. 2000. Gene Ontology: tool for the unification of biology. Nat Genet **25**: 25–29.
648 https://www.nature.com/articles/ng0500_25.

649 Badet T, Oggenfuss U, Abraham L, McDonald BA, Croll D. 2020. A 19-isolate reference-quality
650 global pangenome for the fungal wheat pathogen Zymoseptoria tritici. *BMC Biol* **18**: 12.
651 https://bmcbiol.biomedcentral.com/articles/10.1186/s12915-020-0744-3

652 Barra V, Fachinetti D. 2018. The dark side of centromeres: types, causes and consequences of
653 structural abnormalities implicating centromeric DNA. *Nat Commun* **9**: 4340
654 http://dx.doi.org/10.1038/s41467-018-06545-y

655 Baum M, Sanyal K, Mishra PK, Thaler N, Carbon J. 2006. Formation of functional centromeric
656 chromatin is specified epigenetically in Candida albicans. *Proc Natl Acad Sci* U S A **103**: 14877–
657 14882.

658 Berdan EL, Blanckaert A, Butlin RK, Bank C. 2021. Deleterious mutation accumulation and the long-
659 term fate of chromosomal inversions. *PLOS Genet* **17**: e1009411.
660 http://dx.doi.org/10.1371/journal.pgen.1009411

661 Brimacombe CA, Burke JE, Parsa JY, Catania S, O'meara TR, Witchley JN, Burrack LS, Madhani
662 HD, Noble SM. 2019. A natural histone H2A variant lacking the bub1 phosphorylation site and
663 regulated depletion of centromeric histone CENP-A foster evolvability in candida albicans. *PLoS*
664 *Biol* **17:** 1–21.

665 Burrack LS, Applen SE, Berman J. 2011. The Requirement for the Dam1 Complex Is Dependent upon
666 the Number of Kinetochore Proteins and Microtubules. *Curr Biol* 21**:** 889–896.
667 http://dx.doi.org/10.1016/j.cub.2011.04.002.Burrack LS, Applen Clancey SE, Chacón JM, Gardner
668 MK, Berman J. 2013. Monopolin recruits condensin to organize centromere DNA and repetitive
669 DNA sequences. *Mol Biol Cell* **24**: 2807–2819.

Burrack LS, Hutton HF, Matter KJ, Clancey SA, Liachko I, Plemmons AE, Saha A, Power EA, Turman B, Thevandavakkam MA, et al. 2016. Neocentromeres Provide Chromosome Segregation Accuracy and Centromere Clustering to Multiple Loci along a Candida albicans Chromosome. *PLoS Genet* **12**: 1–24.

Butelli E, Licciardello C, Zhang Y, Liu J, Mackay S, Bailey P, Reforgiato-Recupero G, Martin C. 2012. Retrotransposons control fruit-specific, cold-dependent accumulation of anthocyanins in blood oranges. *Plant Cell* **24**: 1242–1255.

Butler G, Rasmussen MD, Lin MF, Santos MA, Sakthikumar S, Munro CA, Rheinbay E, Grabherr M, Forche A, Reedy JL, et al. 2009. Evolution of pathogenicity and sexual reproduction in eight Candida genomes. *Nature* **459**: 657–662. http://www.nature.com/articles/nature08064

Camacho C, Coulouris G, Avagyan V, Ma N, Papadopoulos J, Bealer K, Madden TL. 2009. BLAST+: Architecture and applications. *BMC Bioinformatics* **10**: 1–9.

Chatterjee N, Shi J, García-Closas M. 2016. Developing and evaluating polygenic risk prediction models for stratified disease prevention. *Nat Rev Genet* **17**: 392–406.

Croll D, Zala M, McDonald BA. 2013. Breakage-fusion-bridge Cycles and Large Insertions Contribute to the Rapid Evolution of Accessory Chromosomes in a Fungal Pathogen ed. J. Heitman. *PLOS Genet* **9**: e1003567. https://dx.plos.org/10.1371/journal.pgen.1003567

Delprat A, Negre B, Puig M, Ruiz A. 2009. The Transposon Galileo Generates Natural Chromosomal Inversions in Drosophila by Ectopic Recombination ed. R. DeSalle. *PLoS One* **4**: e7883. https://dx.plos.org/10.1371/journal.pone.0007883

Devos KM, Brown JKM, Bennetzen JL. 2002. Genome size reduction through illegitimate recombination counteracts genome expansion in Arabidopsis. *Genome Res* **12**: 1075–1079.

Elyashiv E, Bullaughey K, Sattath S, Rinott Y, Przeworski M, Sella G. 2010. Shifts in the intensity of purifying selection: An analysis of genome-wide polymorphism data from two closely related yeast species. *Genome Res* **20**: 1558–1573. http://genome.cshlp.org/lookup/doi/10.1101/gr.108993.110

696 Feurtey A, Lorrain C, McDonald MC, Milgate A, Solomon PS, Warren R, Puccetti G, Scalliet G,
697 Torriani SFF, Gout L, et al. 2023. A thousand-genome panel retraces the global spread and
698 adaptation of a major fungal crop pathogen. *Nat Commun* **14**: 1059.
699 https://www.nature.com/articles/s41467-023-36674-y
700 Forche A, Abbey D, Pisithkul T, Weinzierl MA, Ringstrom T, Bruck D, Petersen K, Berman J. 2011.
701 Stress alters rates and types of loss of heterozygosity in candida albicans. *MBio* **2**: 1–9
702 Forche A, Cromie G, Gerstein AC, Solis N V, Pisithkul T, Srifa W, Jeffery E, Abbey D, Filler SG,
703 Dudley AM, et al. 2018. Rapid Phenotypic and Genotypic Diversification After Exposure to the
704 Oral Host Niche in Candida albicans. *Genetics* **209**: 725–741.
705 https://academic.oup.com/genetics/article/209/3/725/5930940
706 Ford CB, Funt JM, Abbey D, Issi L, Guiducci C, Martinez DA, Delorey T, Li BY, White TC, Cuomo
707 C, et al. 2015. The evolution of drug resistance in clinical isolates of Candida albicans. *Elife* **4**: 1–
708 27. https://elifesciences.org/articles/00662
709 Fouché S, Badet T, Oggenfuss U, Plissonneau C, Francisco CS, Croll D, 2019. Stress-Driven
710 Transposable Element De-repression Dynamics and Virulence Evolution in a Fungal Pathogen,
711 *Mol Biol Evol* **37**: 221—239. https://doi.org/10.1093/molbev/msz216
712 Fouché S, Oggenfuss U, McDonald BA, Croll D. 2023. Recurrent chromosome destabilization through
713 repeat- mediated rearrangements in a fungal pathogen. *bioRxiv*
714 https://doi.org/10.1101/2023.07.14.549097
715 Frahry MB, Sun C, Chong RA, Mueller RL. 2015. Low Levels of LTR Retrotransposon Deletion by
716 Ectopic Recombination in the Gigantic Genomes of Salamanders. *J Mol Evol* **80**: 120–129.
717 http://link.springer.com/10.1007/s00239-014-9663-7
718 Freire-Benéitez V, Price RJ, Buscaino A. 2016. The Chromatin of Candida albicans Pericentromeres
719 Bears Features of Both Euchromatin and Heterochromatin. *Front Microbiol* **7**: 1–11.
720 http://journal.frontiersin.org/Article/10.3389/fmicb.2016.00759/abstract.

González-Sayer S, Oggenfuss U, García I, Aristizabal F, Croll D, Riaño-Pachon DM. 2022. High-quality genome assembly of Pseudocercospora ulei the main threat to natural rubber trees. *Genet Mol Biol* **45**: 1–5. http://www.scielo.br/scielo.php?script=sci_arttext&pid=S1415-47572022000100802&tlng=en

Goodwin TJD, Poulter RTM. 2000. Multiple LTR-retrotransposon families in the asexual yeast Candida albicans. *Genome Res* **10**: 174–191.

Goodwin TJD, Ormandy JE, Poulter RTM. 2001. L1-like non-LTR retrotransposons in the yeast Candida albicans. *Curr Genet* **39**: 83–91.

Guin K, Chen Y, Mishra R, Muzaki SRBM, Thimmappa BC, O'brien CE, Butler G, Sanyal A, Sanyal K. 2020. Spatial inter-centromeric interactions facilitated the emergence of evolutionary new centromeres. *Elife* **9**: 1–28.

Hämälä T, Wafula EK, Guiltinan MJ, Ralph PE, DePamphilis CW, Tiffin P. 2021. Genomic structural variants constrain and facilitate adaptation in natural populations of Theobroma cacao, the chocolate tree. *Proc Natl Acad Sci* **118**: https://pnas.org/doi/full/10.1073/pnas.2102914118

Han S, Dias GB, Basting PJ, Viswanatha R, Perrimon N, Bergman CM. 2022. Local assembly of long reads enables phylogenomics of transposable elements in a polyploid cell line. *Nucleic Acids Res* **50**: e124. 10.1093/nar/gkac794

Harrison BD, Hashemi J, Bibi M, Pulver R, Bavli D, Nahmias Y, Wellington M, Sapiro G, Berman J. 2014. A Tetraploid Intermediate Precedes Aneuploid Formation in Yeasts Exposed to Fluconazole ed. M. Lichten. *PLoS Biol* **12**: e1001815. https://dx.plos.org/10.1371/journal.pbio.1001815

Hartmann FE, Sánchez-Vallet A, McDonald BA, Croll D. 2017. A fungal wheat pathogen evolved host specialization by extensive chromosomal rearrangements. *ISME J* **11**: 1189–1204. http://www.ncbi.nlm.nih.gov/pubmed/28117833

Hartmann FE. 2022. Using structural variants to understand the ecological and evolutionary dynamics of fungal plant pathogens. *New Phytol* **234**: 43–49. https://onlinelibrary.wiley.com/doi/10.1111/nph.17907

747 Hickman MA, Zeng G, Forche A, Hirakawa MP, Abbey D, Harrison BD, Wang YM, Su CH, Bennett
748 RJ, Wang Y, et al. 2013. The “obligate diploid” Candida albicans forms mating-competent
749 haploids. *Nature* **494**: 55–59.
750 Hirakawa MP, Martinez DA, Sakthikumar S, Anderson MZ, Berlin A, Gujja S, Zeng Q, Zisson E,
751 Wang JM, Greenberg JM, et al. 2015. Genetic and phenotypic intra-species variation in Candida
752 albicans. *Genome Res* **25**: 413–425. http://genome.cshlp.org/lookup/doi/10.1101/gr.174623.114
753 Holton NJ, Goodwin TJD, Butler MI, Poulter RTM. 2001. An active retrotransposon in Candida
754 albicans. *Nucleic Acids Res* **29**: 4014–4024.
755 Homolka D, Ivanek R, Capkova J, Jansa P, Forejt J. 2007. Chromosomal rearrangement interferes with
756 meiotic X chromosome inactivation. *Genome Res* **17**: 1431–1437.
757 Ji Y, DeWoody JA. 2016. Genomic Landscape of Long Terminal Repeat Retrotransposons (LTR-RTs)
758 and Solo LTRs as Shaped by Ectopic Recombination in Chicken and Zebra Finch. *J Mol Evol* **82**:
759 251–263.
760 Katoh K, Standley DM. 2013. MAFFT multiple sequence alignment software version 7: Improvements
761 in performance and usability. *Mol Biol Evol* **30:** 772–780.
762 Ketel C, Wang HSW, McClellan M, Bouchonville K, Selmecki A, Lahav T, Gerami-Nejad M, Berman
763 J. 2009. Neocentromeres form efficiently at multiple possible loci in candida albicans. *PLoS Genet*
764 **5**: e1000400. https://dx.plos.org/10.1371/journal.pgen.1000400
765 Koren A, Tsai H, Tirosh I, Burrack LS, Barkai N, Berman J. 2010. Epigenetically-inherited
766 centromere and neocentromere DNA replicates earliest in s-phase. *PLoS Genet* **6**: 15–17.
767 Koren S, Walenz BP, Berlin K, Miller JR, Bergman NH, Phillippy AM. 2017. Canu: scalable and
768 accurate long-read assembly via adaptive k -mer weighting and repeat separation. *Genome Res* **27**:
769 722–736. http://genome.cshlp.org/lookup/doi/10.1101/gr.215087.116
770 Kurtz S, Phillippy A, Delcher AL, Smoot M, Shumway M, Antonescu C, Salzberg SL. 2004. Versatile
771 and open software for comparing large genomes. *Genome Biol* **5**: R12.
772 http://genomebiology.com/2004/5/2/R12

773 Li H, Durbin R. 2009. Fast and accurate short read alignment with Burrows-Wheeler transform.
774 *Bioinformatics* **25**: 1754–1760.
775 Li H, Handsaker B, Wysoker A, Fennell T, Ruan J, Homer N, Marth G, Abecasis G, Durbin R, 1000
776 Genome Project Data Processing Subgroup. 2009. The Sequence Alignment/Map format and
777 SAMtools. *Bioinformatics* **25**: 2078–2079. https://academic.oup.com/bioinformatics/article-
778 lookup/doi/10.1093/bioinformatics/btp352
779 Li H. 2011a. A statistical framework for SNP calling, mutation discovery, association mapping and
780 population genetical parameter estimation from sequencing data. *Bioinformatics* **27**: 2987–2993.
781 https://academic.oup.com/bioinformatics/article/27/21/2987/217423
782 Li H. 2011b. Tabix: fast retrieval of sequence features from generic TAB-delimited files.
783 *Bioinformatics* **27**: 718–719. https://academic.oup.com/bioinformatics/article/27/5/718/262743
784 Li H. 2018. Minimap2: Pairwise alignment for nucleotide sequences. *Bioinformatics* **34**: 3094–3100.
785 Lucek K, Gompert Z, Nosil P. 2019. The role of structural genomic variants in population
786 differentiation and ecotype formation in Timema cristinae walking sticks. *Mol Ecol* **28**: 1224–
787 1237.
788 Ma J, Bennetzen JL. 2004. Rapid recent growth and divergence of rice nuclear genomes. *Proc Natl*
789 *Acad Sci USA* **101**: 12404–12410.
790 MacCallum DM, Castillo L, Nather K, Munro CA, Brown AJP, Gow NAR, Odds FC. 2009. Property
791 Differences among the Four Major Candida albicans Strain Clades. *Eukaryot Cell* **8**: 373–387.
792 https://journals.asm.org/doi/10.1128/EC.00387-08
793 Mahmoud M, Gobet N, Cruz-Dávalos DI, Mounier N, Dessimoz C, Sedlazeck FJ. 2019. Structural
794 variant calling: the long and the short of it. *Genome Biol* **20**: 246.
795 https://genomebiology.biomedcentral.com/articles/10.1186/s13059-019-1828-7
796 Manni M, Berkeley MR, Seppey M, Simão FA, Zdobnov EM. 2021. BUSCO Update: Novel and
797 Streamlined Workflows along with Broader and Deeper Phylogenetic Coverage for Scoring of
798 Eukaryotic, Prokaryotic, and Viral Genomes. *Mol Biol Evol* **38**: 4647–4654.

799 Massonnet M, Vondras AM, Cochetel N, Riaz S, Pap D, Minio A, Figueroa-Balderas R, Walker MA,
800 Cantu D. 2022. Haplotype-resolved powdery mildew resistance loci reveal the impact of
801 heterozygous structural variation on NLR genes in Muscadinia rotundifolia. *G3 Genes, Genomes,*
802 *Genet* **12**: jkac148.
803 https://academic.oup.com/g3journal/article/doi/10.1093/g3journal/jkac148/6607591
804 Matthews GD, Goodwin TJD, Butler MI, Berryman TA, Poulter RTM. 1997. pCal, a highly unusual
805 Ty1/copia retrotransposon from the pathogenic yeast Candida albicans. *J Bacteriol* **179**: 7118–
806 7128.
807 Maxwell PH. 2020. Diverse transposable element landscapes in pathogenic and nonpathogenic yeast
808 models: The value of a comparative perspective. *Mob DNA* **11**: 1–26.
809 Meraldi P, McAinsh AD, Rheinbay E, Sorger PK. 2006. Phylogenetic and structural analysis of
810 centromeric DNA and kinetochore proteins. *Genome Biol* **7**: R23. 10.1186/gb-2006-7-3-r23
811 Mikheenko A, Prjibelski A, Saveliev V, Antipov D, Gurevich A. 2018. Versatile genome assembly
812 evaluation with QUAST-LG. *Bioinformatics* **34**: i142–i150.
813 https://academic.oup.com/bioinformatics/article/34/13/i142/5045727
814 Mishra PK, Baum M, Carbon J. 2007. Centromere size and position in Candida albicans are
815 evolutionarily conserved independent of DNA sequence heterogeneity. *Mol Genet Genomics* **278**:
816 455–465.
817 Muzzey D, Schwartz K, Weissman JS, Sherlock G. 2013. Assembly of a phased diploid Candida
818 albicans genome facilitates allele-specific measurements and provides a simple model for repeat
819 and indel structure. *Genome Biol* **14**: 1–14. 10.1186/gb-2013-14-9-r97
820 Nattestad M, Aboukhalil R, Chin CS, Schatz MC. 2021. Ribbon: intuitive visualization for complex
821 genomic variation. *Bioinformatics* **37**: 413–415.
822 Navarro-García F, Pérez-Diaz RM, Magee BB, Pla J, Nombela C, Magee P t. 1995. Chromosome
823 reorganization in Candida albicans 1001 strain. *J Med Vet Mycol bi-monthly Publ Int Soc Hum*
824 *Anim Mycol* **33**: 361–366.

825 Oggenfuss U, Badet T, Wicker T, Hartmann FE, Singh NK, Abraham L, Karisto P, Vonlanthen T,
826 Mundt C, McDonald BA, Croll D. 2021. A population-level invasion by transposable elements
827 triggers genome expansion in a fungal pathogen. *Elife* **10**: 1–25.
828 https://elifesciences.org/articles/69249.
829 Oggenfuss U, Croll D. 2023. Recent transposable element bursts are associated with the proximity to
830 genes in a fungal plant pathogen. Plos Path 2: 684–696. 10.1371/journal.ppat.1011130
831 Omrane S, Sghyer H, Audeon C, Lanen C, Duplaix C, Walker AS, Fillinger S. 2015. Fungicide efflux
832 and the MgMFS1 transporter contribute to the multidrug resistance phenotype in Zymoseptoria
833 tritici field isolates. *Environ Microbiol* **17**: 2805–2823. 10.1111/1462-2920.12781
834 Omrane S, Audéon C, Ignace A, Duplaix C, Aouini L, Kema G, Walker A-S, Fillinger S. 2017.
835 Plasticity of the MFS1 Promoter Leads to Multidrug Resistance in the Wheat Pathogen
836 Zymoseptoria tritici. *mSphere* **2**: 1–42. https://journals.asm.org/doi/10.1128/mSphere.00393-17
837 Opulente DA, Langdon QK, Buh K V., Haase MAB, Sylvester K, Moriarty R V., Jarzyna M,
838 Considine SL, Schneider RM, Hittinger CT. 2019. Pathogenic budding yeasts isolated outside of
839 clinical settings. *FEMS Yeast Res* **19**: 1–6.
840 Padmanabhan S, Thakur J, Siddharthan R, Sanyal K. 2008. Rapid evolution of Cse4p-rich centromeric
841 DNA sequences in closely related pathogenic yeasts, Candida albicans and Candida dubliniensis.
842 *Proc Natl Acad Sci USA* **105**: 19797–19802.
843 Potocki L, Kuna E, Filip K, Kasprzyk B, Lewinska A, Wnuk M. 2019. Activation of transposable
844 elements and genetic instability during long-term culture of the human fungal pathogen Candida
845 albicans. *Biogerontology* **20**: 457–474. https://doi.org/10.1007/s10522-019-09809-2.
846 Quinlan AR, Hall IM. 2010. BEDTools: A flexible suite of utilities for comparing genomic features.
847 *Bioinformatics* **26**: 841–842.
848 R Core Team. 2023. R: A language and environment for statistical computing. R Foundation for
849 Statistical Computing, Vienna, Austria. https://www.R-project.org/

Rausch T, Zichner T, Schlattl A, Stütz AM, Benes V, Korbel JO. 2012. DELLY: Structural variant discovery by integrated paired-end and split-read analysis. *Bioinformatics* **28**: 333–339.

Rice P, Longden L, Bleasby A. 2000. EMBOSS: The European Molecular Biology Open Software Suite. *Trends Genet* **16**: 276–277.

Rogers PD, Barker KS. 2003. Genome-wide expression profile analysis reveals coordinately regulated genes associated with stepwise acquisition of azole resistance in Candida albicans clinical isolates. *Antimicrob Agents Chemother* **47**: 1220–1227.

Ropars J, Maufrais C, Diogo D, Marcet-Houben M, Perin A, Sertour N, Mosca K, Permal E, Laval G, Bouchier C, et al. 2018. Gene flow contributes to diversification of the major fungal pathogen Candida albicans. *Nat Commun* **9**: 2253. https://www.nature.com/articles/s41467-018-04787-4

Rustchenko-Bulgac EP. 1991. Variations of Candida albicans electrophoretic karyotypes. *J Bacteriol* **173**: 6586–6596.

Sanyal K, Baum M, Carbon J. 2004. Centromeric DNA sequences in the pathogenic yeast Candida albicans are all different and unique. *Proc Natl Acad Sci USA* **101**: 11374–11379.

Selmecki A, Bergmann S, Berman J. 2005. Comparative genome hybridization reveals widespread aneuploidy in Candida albicans laboratory strains. Mol Microbiol **55**: 1553–1565.

Selmecki A, Forche A, Berman J. 2006. Aneuploidy and Isochromosome Formation in Drug-Resistant Candida albicans. *Science* **313**: 367–370.

Selmecki A, Gerami-Nejad M, Paulson C, Forche A, Berman J. 2008. An isochromosome confers drug resistance in vivo by amplification of two genes, ERG11 and TAC1. *Mol Microbiol* **68**: 624–641.

Selmecki AM, Dulmage K, Cowen LE, Anderson JB, Berman J. 2009. Acquisition of Aneuploidy Provides Increased Fitness during the Evolution of Antifungal Drug Resistance ed. H.D. Madhani. *PLoS Genet* **5**: e1000705. https://dx.plos.org/10.1371/journal.pgen.1000705

Shih J, Sarmashghi S, Zhakula-Kostadinova N, Zhang S, Georgis Y, Hoyt SH, Cuoco MS, Gao GF, Spurr LF, Berger AC, et al. 2023. Cancer aneuploidies are shaped primarily by effects on tumour fitness. *Nature* **619**: 793–800. https://www.nature.com/articles/s41586-023-06266-3.

Simão FA, Waterhouse RM, Ioannidis P, Kriventseva E V., Zdobnov EM. 2015. BUSCO: Assessing genome assembly and annotation completeness with single-copy orthologs. *Bioinformatics* **31:** 3210–3212.

Stamatakis A. 2014. RAxML version 8: A tool for phylogenetic analysis and post-analysis of large phylogenies. *Bioinformatics* **30**: 1312–1313.

Stritt C, Gordon SP, Wicker T, Vogel JP, Roulin AC. 2017. Recent activity in expanding populations and purifying selection have shaped transposable element landscapes across natural accessions of the Mediterranean grass Brachypodium distachyon. *Genome Biol Evol* 10: 1–38. http://academic.oup.com/gbe/advance-article/doi/10.1093/gbe/evx276/4769669.

Stritt C, Thieme M, Roulin AC. 2021. Rare transposable elements challenge the prevailing view of transposition dynamics in plants. *Am J Bot* **8**: 1310-1314.

Talbert PB, Bryson TD, Henikoff S. 2004. Adaptive evolution of centromere proteins in plants and animals. *J Biol* **3**: 18. http://jbiol.com/content/3/4/18

The Gene Ontology Consortium, Ashburner M, Ball CA, Blake JA, Botstein D, Butler H, Cherry JM, Davis AP, Dolinski K, Dwight SS, et al. 2000. Gene Ontology: Tool for the unification of biology. Nat Genet 25: 25-29.

Thorvaldsdóttir H, Robinson JT, Mesirov JP. 2013. Integrative Genomics Viewer (IGV): High-performance genomics data visualization and exploration. *Brief Bioinform* **14**: 178–192.

Todd RT, Wikoff TD, Forche A, Selmecki A. 2019. Genome plasticity in Candida albicans is driven by long repeat sequences. *Elife* **8**: 1–33. https://elifesciences.org/articles/45954

Todd RT, Selmecki A. 2020. Expandable and reversible copy number amplification drives rapid adaptation to antifungal drugs. *Elife* **9**: 1–33. https://elifesciences.org/articles/58349

Todd RT, Soisangwan N, Peters S, Kemp B, Crooks T, Gerstein A, Selmecki A. 2023. Antifungal drug concentration impacts the spectrum of adaptive mutations in Candida albicans. *Mol Biol Evol* **40**: 1–33. https://doi.org/10.1093/molbev/msad009

Tsai H-J, Baller JA, Liachko I, Koren A, Burrack LS, Hickman MA, Thevandavakkam MA, Rusche LN, Berman J. 2014. Origin Replication Complex Binding, Nucleosome Depletion Patterns, and a Primary Sequence Motif Can Predict Origins of Replication in a Genome with Epigenetic Centromeres. *MBio* **5**: 1–9 https://journals.asm.org/doi/10.1128/mBio.01703-14.

Van het Hoog M, Rast TJ, Martchenko M, Grindle S, Dignard D, Hogues H, Cuomo C, Berriman M, Scherer S, Magee BB, et al. 2007. Assembly of the Candida albicans genome into sixteen supercontigs aligned on the eight chromosomes. *Genome Biol* **4**: R52. http://genomebiology.biomedcentral.com/articles/10.1186/gb-2007-8-4-r52

Vande Zande P, Zhou X, Selmecki A. 2023. The Dynamic Fungal Genome: Polyploidy, Aneuploidy and Copy Number Variation in Response to Stress. *Annu Rev Microbiol* **77**: 341–361. https://www.annualreviews.org/doi/10.1146/annurev-micro-041320-112443.

Vanden Bossche H, Marichal P, Odds FC. 1994. Molecular mechanisms of drug resistance in fungi. *Trends Microbiol* **2**: 393–400. https://linkinghub.elsevier.com/retrieve/pii/0966842X94906181

Wang LG, Lam TTY, Xu S, Dai Z, Zhou L, Feng T, Guo P, Dunn CW, Jones BR, Bradley T, et al. 2020. Treeio: An R Package for Phylogenetic Tree Input and Output with Richly Annotated and Associated Data. *Mol Biol Evol* **37**: 599–603.

Waterhouse AM, Procter JB, Martin DMA, Clamp M, Barton GJ. 2009. Jalview Version 2—a multiple sequence alignment editor and analysis workbench. *Bioinformatics* **25**: 1189–1191. https://academic.oup.com/bioinformatics/article/25/9/1189/203460

Wells JN, Feschotte C. 2020. A Field Guide to Transposable Elements. *Annu Rev Genet* 54: 7–34.

White TC, Marr KA, Bowden RA. 1998. Clinical, Cellular, and Molecular Factors That Contribute to Antifungal Drug Resistance. *Clin Microbiol Rev* **11**: 382–402. https://journals.asm.org/doi/10.1128/CMR.11.2.382

924 Wick RR, Judd LM, Holt KE. 2019. Performance of neural network basecalling tools for Oxford
925 Nanopore sequencing. *Genome Biol* **20**: 129.
926 https://genomebiology.biomedcentral.com/articles/10.1186/s13059-019-1727-y
927 Wicker T, Sabot F, Hua-Van A, Bennetzen JL, Capy P, Chalhoub B, Flavell A, Leroy P, Morgante M,
928 Panaud O, et al. 2007. A unified classification system for eukaryotic transposable elements. *Nat*
929 *Rev Genet* **8**: 973–982.
930 Wickham H. 2016. ggplot2: Elegant Graphics for Data Analysis. Springer-Verlag, New York
931 https://ggplot2.tidyverse.org
932 Wu W, Lockhart SR, Pujol C, Srikantha T, Soll DR. 2007. Heterozygosity of genes on the sex
933 chromosome regulates Candida albicans virulence. *Mol Microbiol* **64**: 1587–1604.
934 Yang Z, Ge X, Yang Z, Qin W, Sun G, Wang Z, Li Z, Liu J, Wu J, Wang Y, et al. 2019. Extensive
935 intraspecific gene order and gene structural variations in upland cotton cultivars. *Nat Commun* **10**:
936 2989. http://dx.doi.org/10.1038/s41467-019-10820-x
937 Yu G, Smith DK, Zhu H, Guan Y, Lam TTY. 2017. Ggtree: an R Package for Visualization and
938 Annotation of Phylogenetic Trees With Their Covariates and Other Associated Data. *Methods*
939 *Ecol Evol* **8**: 28–36.
940 Yu G, Lam TTY, Zhu H, Guan Y. 2018. Two methods for mapping and visualizing associated data on
941 phylogeny using GGTree. *Mol Biol Evol* **35**: 3041–3043.
942 Yu G. 2020. Using ggtree to Visualize Data on Tree-Like Structures. *Curr Protoc Bioinforma* **69**: e96.
943 https://currentprotocols.onlinelibrary.wiley.com/doi/10.1002/cpbi.96
944 Zhu C, Yan L, Wang X, Miao Q, Li X, Yang F, Cao Y, Gao P, Bi X, Jiang Y. 2014. Transposition of
945 the Zorro2 Retrotransposon Is Activated by Miconazole in Candida albicans. *Biol Pharm Bull* **37**:
946 37–43. https://www.jstage.jst.go.jp/article/bpb/37/1/37_b13-00508/_article